

Materials Science Forum Vol 514-516, pp. 23 (2006)

MICROSTRUCTURE AND THERMAL FEATURES OF a-Si:H AND nc-Si:H THIN FILMS PRODUCED BY r.f. SPUTTERING

V.Thaiyalnayaki, M. F. Cerqueira, F. Macedo, J. A. Ferreira

Departamento de Física, Universidade do Minho, 4710-057 Braga, Portugal

Keywords: Nanocrystalline silicon, Thermal properties, structure

Summary: Amorphous and nanocrystalline silicon thin films have been produced by reactive r.f. sputtering and their microstructure, optical and thermal properties were evaluated. A good correlation was found between the microstructure determined by Raman spectroscopy and X-ray diffraction and the thermal transport parameters.

1 Introduction

Modern growth techniques have shown the ability to produce semiconductor nano-structures (typical size $< 10\text{ nm}$), with spatial confinement of electrons in all three dimensions [1, 2]. These systems are of considerable interest because of the new physics involved and potential device applications in the area of Si-based optoelectronics [3, 4]. Indeed, a size-dependent photoluminescence (PL) in the visible spectral range has been observed from Si NC's grown inside SiO_2 , indicating the quantized nature of their electronic spectra.

Optical properties (e. g. band gap) and heat dissipation characteristics are important parameters for the performance of devices, the first one related with absorption features and the last one is related to the technological tendency of reducing the physical size of the devices. We have produced and studied amorphous and nanocrystalline silicon thin films, in order to evaluate the effect of the film microstructure on their thermal and optical properties, and to get the expected properties for the required applications.

2 Experimental

The nanocrystalline (nc-Si:H) silicon thin films were grown by reactive by r.f. reactive magnetron sputtering in an Ar/H_2 atmosphere on ordinary glass and crystalline silicon substrates under different growth conditions (r.f power (P), substrate temperature (T), applied bias and gas mixture composition: hydrogen (P_{H_2}) and argon (P_{Ar})) applying a similar

procedure to that used for the preparing $\mu\text{c-Si:H}$ films [5]. The target used was c-Si of high purity (99.99%). The substrate-target distance was fixed to 55 mm.

Samples with different structural parameters, i.e., different crystalline fraction and crystallite grain sizes, were obtained by varying the growth parameters. Additionally an amorphous film was also obtained. The films growth conditions are presented in Table 1. In the growth procedure we have used a H_2 rich atmosphere (Table 1), once the role of atomic hydrogen is to etch preferentially the amorphous phase and promote the amorphous-to-crystalline transition [6, 7].

The structural characterization was performed by standard micro-Raman spectroscopy under excitation with 514.5nm Ar^+ -laser line and by the X-ray diffractometry in the grazing incidence geometry.

To analyse the Raman spectra, computer simulation was used, considering the spectral profile as a superposition of the amorphous spectrum and the crystalline spectrum. The crystalline profile was calculated based on the Strong Phonon Confinement (SPC) [8] and a Gaussian profile was attributed to the amorphous transverse optical mode (TO) structure. To determine the crystalline volume fraction, C, we have used:

$$C = \frac{I_c}{I_c + I_a (0.1 + e^{-D/25})}$$

where I_c is the integrated intensity of the crystalline component, I_a the integrated intensity of the amorphous peak. D (nm), the average size of the crystallites has also been taken into account once it can influence the value of the scattering cross section.

Table 1 - Growth conditions for nanocrystalline silicon thin films

Sample	T (°C)	RF (W)	P_{H_2} (Pa)	P_{Ar} (Pa)	Bias (V)
Si 47	400	150	0.23	0.20	
Si 51	300	80	0.39	0.12	
Si 52	150	150	0.39	0.12	
Si 53	300	80	0.39	0.12	-50
Si 54	400	80	0.16	0.12	

By fitting the c-Si (111) peak to the X-Ray spectra using a Pseudo-Voigt [9] function we have obtained information on the average crystal size, D, and on the crystal strain, ϵ , according to:

$$D = \lambda / \beta_C \cos \theta;$$

$$\varepsilon = \beta_G / 4 \tan \theta$$

where β_C and β_G are the integral breadths of the Cauchy and Gauss components, respectively.

The thermal diffusivity (α) values were obtained by the photothermal beam deflection method (fig. 1). In this technique [10] the deflection of a probe beam, skimming or bouncing the sample surface is measured and related to the thermal properties of the sample. This deflection (ϕ) is caused by surface temperature oscillations as a consequence of excitation of the sample with a modulated laser beam:

$$\phi(r, t) = \frac{1}{n} \frac{\partial n}{\partial T} \int \nabla T(r, t) dl$$

where l is the optical path length and n is the surrounding medium refractive index.

In order to calculate the thermal diffusivity, we measured the amplitude and phase of the transverse component of the deflection vector [11]:

$$\phi_t = \frac{1}{n} \frac{\partial n}{\partial T} \int_{-\infty}^{\infty} \frac{\partial T}{\partial x} dy$$

Thermal diffusivity values were obtained by fitting the solutions of the equation above to the experimental data, being α one of the fitting parameters.

As the penetration depth can be changed by varying the modulation frequency, this technique is specially indicated for thin films and coatings [12].

3 Results and discussion

Raman spectroscopy, being a very sensitive technique, detects details of the microstructure. The Stokes peak in the vicinity of 521 cm^{-1} is generally attributed to the transverse optical mode of crystalline silicon. The peak is shifted to smaller wave numbers as the crystal diameter decreases due to the confinement effects. Amorphous silicon in Raman is characterized by a band near 480 cm^{-1} .

Figure 2 shows the Raman spectra for the nc-Si:H samples studied. The broad band (at around 480 cm^{-1}) is related to the silicon amorphous matrix and is present in the spectra of all

samples. The nanocrystalline samples show another contribution in the Raman spectra (narrow peak) related to the presence of crystallites. The crystallinity of the samples is obtained by using the intensity ratio of the Stokes peaks at 480 cm^{-1} and at 521 cm^{-1} .

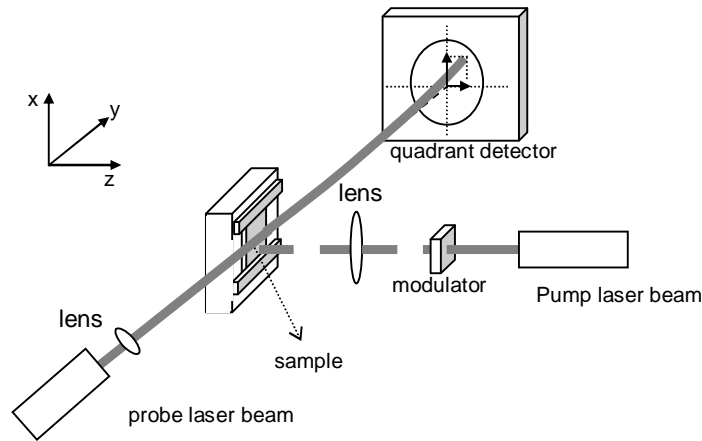


Fig 1 - Schematic view of the experimental setup using air as surrounding medium. The pump laser is an Ar⁺ laser and the probe beam a low power HeNe laser.

Information on the crystalline fraction and on the average crystallite size of Si nanocrystals is obtained by using the X-ray technique combined with Raman spectroscopy. The results are presented in table 2.

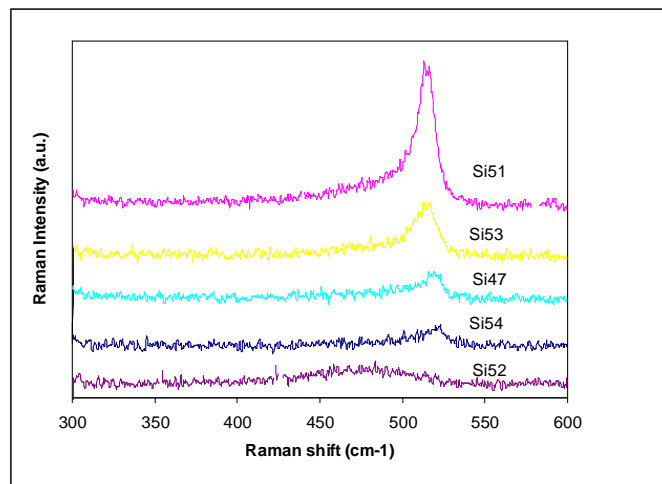


Fig 2 - Raman spectra of some nanocrystalline and amorphous samples.

Table 2 - Structural and optical parameters for the silicon thin films under study

Sample	D (nm)	C (%)	Eg (eV)	d (nm)
Si 47	7.2	65	1.8	1166
Si 51	6.0	50	2.2	<500
Si 52	-	0	1.7	3800
Si 53	6.5	69	1.8	<500
Si 54	8.0	66	1.9	2500

For optical characterization and determination of thickness we have analyzed the transmission spectra in the visible and near infrared (IR) range, according to the Swanepoel method [13]. Using Tauc's plot [14] to the absorption coefficient we have obtained the energy gap (Eg). The results are presented in table 2 together with the structural parameters. In figure 3 we present the optical density of our films. From figure 3 we can observe that the transition in the optical density is very pronounced in the amorphous sample (Si52) and it becomes less abrupt for the nanocrystallines samples. For these samples the transition has become almost flat for smaller crystal sizes (for instance from Si53 to Si51). It is also visible that the energy gap (from Tauc's plot) is higher for the sample having the smallest crystal size.

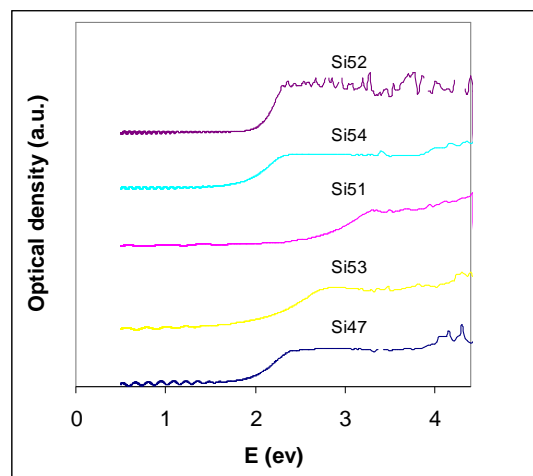


Fig 3 – Optical density of some nanocrystalline and amorphous samples.

In table 3 the thermal parameters for two samples, one hydrogenated amorphous silicon and the other nanocrystalline silicon with an average crystal size of 72 Å, are shown. We can see that the measured thermal diffusivity values increase as the modulation frequency increases. This behaviour can be explained since for low frequencies we are deep in the substrate, which has a much lower diffusivity ($8 \times 10^{-7} \text{ m}^2/\text{s}$) than that of the sample. The values for the highest

frequency used should be considered as the film thermal diffusivity. For the thinner sample (Si 47) the values tend to decrease faster, as the sample becomes thermally thin. Then, if we compare the diffusivity of the two samples at the higher frequency we can conclude that the diffusivity is higher for the nanocrystalline sample, which means that the presence of nanocrystals increases the diffusivity of the sample. This behaviour is in accordance with previously reported results [15] for this kind of materials.

Table 3 - Thermal diffusivity obtained for two silicon thin films under study

Sample	Si 52 (amorphous)	Si 47 (nanocrystalline)
Modulation frequency (Hz)	Thermal Diffusivity ($\times 10^{-5} \text{ m}^2/\text{s}$)	
73	4.6	1.7
423	5.1	3.4
3200	6.6	4.1
5200	6.5	7.4

4 Conclusions

It was shown in this work that the nanocrystalline silicon becomes a material with a great potential for practical applications due to the enhancement of its optical properties when compared with amorphous silicon and due to the possibility of being applied to engineering by controlling the deposition parameters.

We have shown the ability to produce amorphous and nanocrystalline thin films by r.f. sputtering at substrates temperatures lower than 400°C.

We can see from fig 3 that the amorphous sample shows a much more pronounced transition when compared with the nanocrystalline ones. In accordance with theory, we have obtained an increase of the Tauc energy for the nanocrystalline samples, as the crystalline size decreases.

Thermal transport properties of amorphous and nanocrystalline silicon samples have been measured. The measurements at high frequencies don't include the substrate contribution and then we can measure only the thermal diffusivity of the film. We verify that the thermal diffusivity of the nanocrystalline film is higher than that of the amorphous film. The thermal analysis done indicates a direct dependence between thermal properties and structural parameters. Thermal diffusivity obtained for the samples under study are in good agreement with the values found in literature for a-Si and c-Si bulk material.

Acknowledgement: This work was supported by FCT Project POCTI / CTM / 39395 / 2001

References

- [1] – M.I.Vasilevskiy, Phys. Rev. B 66, 195326 (2002)
- [2] – M.I.Vasilevskiy, E.V.Anda and S.S.Makler, Phys. Rev. B 70, 035318 (2004)
- [3] – F. Iacona, G. Franzò and C. Spinella, J. Appl. Phys. 87, 1295 (2000)
- [4] – J. Linnros, N. Lalic, A. Galeckas and V. Grivickas, J. Appl. Phys. 86, 6128 (1999)
- [5] – Cerqueira M.F., Andritschky M. et al., Vacuum. 46, 1385 (1995)
- [6] – P. Alpuim, V. Chu, J.P. Conde, J. Appl. Phys. 86, 3812 (1999)
- [7] – M.F. Cerqueira, J.A. Ferreira, G.J Adriaenssens, Thin Solid Films, 370, 128 (2000)
- [8] – I. Campbell and P. M. Fauchet, Solid State Commun., 58, 739 (1986)
- [9] – Th. H. de Keijser, J. I. Langdord, E. F. Mittemeijer and A. B. P. Vogels, J. Appl. Crystallogr., 15, 308 (1982)
- [10] – Boccara A. C., D. Fournier and J. Badoz, Appl. Phys. Lett., 37, 130 (1980)
- [11] – A. Salazar, A. Sánchez-Lavega, and J. Fernández, J. Appl. Phys., 65, 4150 (1989).
- [12] – Z. L. Wu, P. K. Kuo, Lanhua Wei, S. L. Gu and R. L. Thomas, Thin Solid Films, 236, 191 (1993)
- [13] – R. Swanepoel, J. Phys., E16, 1214 (1983)
- [14] – J. Tauc, “Optical Properties of Solids”, ed. F. Abeles (Amsterdam: North-Holland) (1972)
- [15] – Lanhua Wei, Mark Vaudin, Cheol Song Hwang, and Grady White, J. Mater. Res., Vol 10, 1889 (1995)